Combined crossed molecular beams and *ab initio* investigation of the formation of carbon-bearing molecules in the interstellar medium *via* neutral–neutral reactions

R. I. Kaiser,[a]**† C. Ochsenfeld,**[b]**‡ D. Stranges,**[c]**§ M. Head-Gordon,**[b]**¶ Y. T. Lee**[d]******

[a] *Academia Sinica, Institute of Atomic and Molecular Sciences, 1, Section 4, Roosevelt Rd.,Taipei, 116, Taiwan, ROC, and Department of Physics, Technical University Chemnitz-Zwickau, 09107 Chemnitz, Germany*

[b] *Department of Chemistry, University of California, Berkeley, California, 94720, USA, and Chemical Sciences Division, Lawrence Berkeley National Laboratory, Berkeley, California, 94720, USA*

[c] *Dipartimento di Chimica (NEC), Universita La Sapienza, Piazzale, A. Moro 5, 00185 Rome, Italy, and Centro Stadi, Termodinamica Chimica Alte Temperature, CNR, 00185 Rome, Italy*

[d] *Academia Sinica, Institute of Atomic and Molecular Sciences, 1, Section 4, Roosevelt Rd., Taipei, 116, Taiwan, ROC*

The crossed molecular beams reaction of atomic carbon $C(^3P_j)$ with hydrogen sulfide, H_2S, allene, H_2CCCH_2, the vinyl radical, C_2H_3, and deuteroacetylene, C_2HD, have been studied at different collision energies up to 42.2 kJ mol^{-1} and combined with high level *ab initio* calculations. All reactions are barrier-less and are dominated by a carbon–hydrogen exchange to form thioformyl (HCS), butatrienyl (HCCCCH$_2$), C_3H_2 isomer(s), and deuteriated tricarbon hydride(s). This carbon–hydrogen replacement channel represents a one-step alternative reaction pathway to competing ion–molecule reactions to form complex, carbon-bearing molecules in the interstellar medium as well as in the outflow of carbon stars.

1 Introduction

One of the most fundamental questions in astrochemistry is the formation of molecules in the interstellar medium (ISM). To tackle this still unresolved puzzle, we have first to familiarize ourselves with the physical conditions and the distribution of matter in distinct interstellar environments before we can elucidate well defined mechanisms to synthesize interstellar molecules and radicals.

The ISM contains *ca.* 10% of the mass of our galaxy and consists of gas (99%) and 0.1–0.2 µm, ellipsoidal-shaped grain particles (1%) with averaged number densities of 1 H atom cm^{-3} and 10^{-11} grains cm^{-3}, respectively.[1] Its chemical composition is dominated by hydrogen and helium (93.38% H, 6.49% He), whereas biogenic elements oxygen, carbon, and nitrogen contribute 0.11% (O : C : N $\approx$ 8 : 3 : 1).[2] All remaining elements furnish only 0.02%. Although the interstellar dust component embodies only 1%, these predominantly silicate- and carbonaceous-based grain nuclei play a key role in the

† E-mail: kaiser@po.iams.sinica.edu.tw
‡ E-mail: chi@alcatraz.cchem.berkeley.edu
§ E-mail: dstranges@axrma.uniromal.it
¶ E-mail: mhg@alcatraz.cchem.berkeley.edu
** E-mail: ytlee@gate.sinica.edu.tw

formation of new molecules. Deep in the interior of dense clouds, grain particles effectively shield newly synthesized molecules in the gas phase from the destructive external galactic UV radiation field. In addition, these grains hold typical temperatures of 10 K in dark clouds.[3] Molecules, radicals and atoms from the gas phase are accreted on grain surfaces resulting in an icy mantle up to 0.1 μm thick. Here, solid mixtures containing H_2O, CO, CH_3OH, NH_3, H_2S, CH_4, H_2CO, OCS, OCN^-, H_2, and CO_2 have been identified unambiguously *via* IR spectroscopy.[4] This ice mantle is altered chemically by the cosmic-ray-induced internal UV radiation present even in the deep interior of dense clouds[5] and through charged particles such as protons (p, H^+) and helium nuclei (α-particles, He^{2+})[6] of the galactic cosmic radiation field. This combined photon and particle bombardment leads to the synthesis of new molecules in the solid state.[7] Since typical carbon–hydrogen and carbon–carbon bond strengths in organic molecules range between 3 and 10 eV, cosmic ray particles are too energetic to form stable chemical bonds as implanted into the icy mantle. However, upon interaction with the solid target, each cosmic ray particle releases its excess energy to the target atoms in successive collisions *via* elastic and inelastic interactions.[8] Here, the elastic process transfers energy to the nuclei of the target atoms igniting primary knock-on particles (PKOs; first generation of knock-on particles) if this amount is larger than the binding energy of the atom. MeV α-particles, for example, generate carbon PKOs with kinetic energies up to 10 keV. These knock-on particles can transfer their energy in consecutive encounters to the target atoms, resulting in a collision cascade of secondary, tertiary *etc.*, knock-on atoms. Moderated to *ca.* 1–10 eV, the so-called chemical energy range, these atoms are not in thermal equilibrium with the 10 K target (hence: non-equilibrium or suprathermal particles) and react with the target molecules *via* elementary steps of bond insertion, addition to double or triple bonds, and hydrogen abstraction.[9] Irradiating solid CH_4, C_2H_2, and C_2H_4 samples with MeV particles leads to a broad product spectrum of synthesized species such as atomic and molecular hydrogen, H and H_2, CH_n ($n = 1$–4), C_2H_n ($n = 1$–6), C_3H_n ($n = 4$–8), larger alkanes and alkenes with up to 18 carbon atoms, as well as polycyclic aromatic hydrocarbons (PAHs) up to coronene.[10] The power of these suprathermal reactions to form new molecules at temperatures even as low as 10 K is based in their ability to overcome reaction barriers in the entrance channel easily, since suprathermal species can impart their excess kinetic energy into the transition state of the reaction. Even endothermic reactions are feasible if the energy deficit can be covered by a suprathermal reactant, extending the synthetic power of this reaction class beyond thermal reactions and diffusion controlled chemistry on interstellar grains. These unique aspects of suprathermal reactions result in reaction rate constants up to 16 orders of magnitude larger than their thermal counterparts, even at temperatures as low as 10 K.[11] Once molecules are formed on interstellar grains, a consecutive grain heating by a young stellar object embedded inside dense clouds, followed by equilibrium sublimation, as well as explosive molecule ejections from grains storing a critical concentration of radicals, can redistribute these molecules into the gas phase.[12]

Besides the solid state, molecules can also be synthesized in the gas phase of the ISM. Table 1 lists those species detected so far, most of them thermally unstable and extremely reactive in terrestrial laboratories.[13] On average, 97% of all species exist as neutrals, whereas only 3% are ions. These molecules, radicals and ions are not distributed homogeneously, but are confined to distinct interstellar environments such as interstellar clouds, hot cores, and circumstellar envelopes of, *e.g.* dying carbon and oxygen stars.[1,2] Diffuse (hot) clouds hold number densities n of *ca.* 10 molecules cm^{-3} and average translational temperatures $T \approx 100$ K, whereas dense (cold, dark, molecular) clouds are characterized by $n = 10^2$–10^6 molecules cm^{-3} and $T = 10$–40 K. Hot cores of molecular clouds have typical number densities up to 10^7 molecules cm^{-3} and temperatures reaching up to 200 K. Molecules in the outflow of carbon stars contribute only a minor amount to the interstellar matter, but temperatures can rise up to 4000 K

Table 1 Classification of neutral molecules, radicals, and ions detected in the ISM '?' indicates an uncertain assignment; bold typed species are only detected in circumstellar environments

diatomic molecules
H_2

1st atom	group 4			group 5		
2nd atom	group 4	group 5	group 6	group 4	group 5	group 6
1st period	CC	CN	CO	NC		NO
2nd period	**CSi**	**CP**	CS	**NSi**	NP	NS
1st period	**SiC**	**SiN**	SiO	**PC**	PN	
2nd Period			SiS			

1st atom	group 6		
2nd atom	group 4	group 5	group 6
1st period	OC	ON	OS
2nd period	OSi		
1st period	SC	SN	SO
2nd Period	SSi		

halides and pseudohalides

HCl	NaCl	KCl	NaCN
	MgCN	**MgNC**	
	AlF	**AlCl**	

hydrides

CH_4	NH_3	H_2O	CH	NH	OH
SiH_4		H_2S	CH_2	NH_2	
		SiH_2(?)			

closed-shell hydroarbons

CH_4 **C_2H_4** C_2H_2 $CH_3C{\equiv}CH$ $CH_3C{\equiv}C-C{\equiv}CH$

ring molecules

C_2H_4O **SiC_2** C_3H C_3H_2

long-chain molecules

$CH_3-(C{\equiv}C)_n-H$	$n = 1, 2$
HC_n	$n = 0-8$
C_n	$n = 2, 3, 5$
$H-(C{\equiv}C)_n-CN$	$n = 0-4$
$-(C{\equiv}C)_n-CN$	$n = 0, 1$
$CH_3-(C{\equiv}C)_n-CN$	$n = 0, 1, 2$
H_2C_n	$n = 3, 4$
C_nO	$n = 1, 2, 3, 5(?)$
C_nS	$n = 1, 2, 3, 5$
C_nSi	$n = 4$
HCCNC	
HNCCC	

Table 1   *Continued*

structural isomers

c-C_3H_2	l-C_3H_2
c-C_3H	l-C_3H
HCN	HNC
CH_3CN	CH_3NC
MgCN	MgNC
HCO	HOC
HCCCN	HCCNC
HCO^+	HOC^+

oxygen- and carbon-containing neutral molecules

CH_3—OH	H_2C=O	HCOOH
C_2H_5—OH	CH_3—CHO	CH_3—COOH
	$HCOOCH_3$	

$$H_2C=C=O \quad HCC—CHO \quad CH_3—CO—CH_3 \quad CH_3—O—CH_3$$
$$CO \qquad CO_2 \qquad HOC \qquad HOC \qquad C_2O \qquad C_3O \qquad C_5O(?)$$

sulfur- and carbon-containing neutral molecules

$$CH_3—SH \qquad H_2C=S \qquad CS$$

nitrogen- and carbon-containing neutral molecules

HCN	**CH—CN**			
	CH_2—CN			
	CH_3CN	C_2H_3—CN	C_2H_5—CN	H_2N—CN
CH_3—NH_2	H_2C=NH			
	H_2C=N			

other neutral molecules

	SO_2	OCS	N_2O	HNO
HCO—NH_2	HN=C=O		HN=C=S
H_2N—CH_2—COOH			

ions

$$CH^+ \qquad CO^+ \qquad CS^+ \qquad SO^+$$
$$HCO^+ \quad HCS^+ \quad HNN^+ \quad HOC^+ \quad H_3^+$$
$$HCNH^+ \qquad HOCO^+ \qquad CH_2D^+ \qquad H_3O^+$$
$$H_2COH^+ HC_3NH^+$$
$$C_{60}^+(?)$$

in the outer photosphere[14] and a more complex chemistry is anticipated. Comparing this data with that from terrestrial laboratories, it is worth mentioning that number densities even in the 'densest' interstellar clouds of 10^6 molecules cm^{-3} and $T = 40$ K are equivalent to 5×10^{-12} mbar, which compares to the best ultra-high vacuum (UHV) condition in terrestrial laboratories.

However, despite large fractional abundances of, *e.g.* C_3H and C_3H_2, up to 10^{-8} relative to atomic hydrogen, well defined synthetic mechanisms, even of these abundant
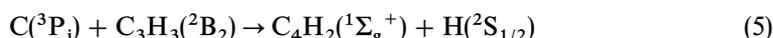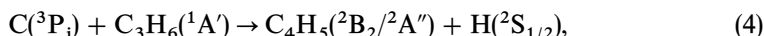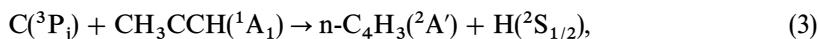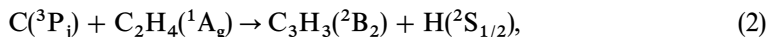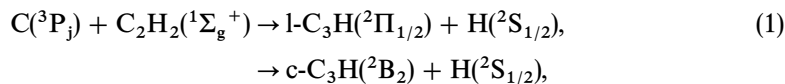
species, have not yet been fully resolved. Since the kinetic energy of interstellar species is confined to typically 0.8 kJ mol^{-1} (diffuse clouds) and 0.08 kJ mol^{-1} (dark, molecular clouds) on average, gas-phase reactions under thermodynamical equilibrium conditions (a) must be exothermic or only slightly endothermic, (b) should exhibit little or no entrance barriers and (c) must involve only two-body collisions. A three-body reaction occurs only once in a few 10^9 years and can be neglected since mean interstellar cloud lifetimes are *ca.* 10^6 years. Early chemical equilibrium models of interstellar chemistry satisfy these criteria and focus on ion–molecule reactions, radiative associations, and dissociative recombination between cations and electrons to advance interstellar chemistry.[15] This approach, however, involves multiple reaction chains with subsequent collisions, and often cannot reproduce observed structural isomer ratios, isotopic enrichments, and number densities of extremely abundant radicals, *e.g.* those of C_3H and C_3H_2. The inclusion of alternative, one-step, exothermic neutral–neutral reactions into chemical models of the circumstellar envelope surrounding the carbon star IRC+10216 and the dark cloud TMC-1 occurred only gradually,[16] predominantly because entrance barriers were assumed to hinder this reaction class. However, the *ad hoc* postulation of spin conservation, simple thermochemistry, and the lack of information on reaction products, clearly demonstrate the urgency of systematic laboratory examinations probing detailed chemical dynamics and reaction products of neutral–neutral encounters in the gas phase of the ISM.

Recently, Husain and co-workers investigated rate constants of $C(^3P_j)$ with unsaturated hydrocarbons monitoring the decay kinetics of $C(^3P_j)$ at room temperature.[17] These bulk experiments indicated that the reactions proceed with second-order kinetics, are barrier-less, and rapid ($k = 10^{-10}$–10^{-9} cm^3 s^{-1}) within orbiting limits.[18] Likewise, kinetic studies of neutral–neutral reactions involving OH, CN, and CH radicals at ultra-low temperatures revealed rate constants of *ca.* $(1$–6×10^{-10} cm^3 s^{-1} with maxima between 50 and 70 K, and only a slight decrease as the temperature falls to 13 K.[19] However, despite extremely valuable kinetic data, it was not possible to probe the reaction products experimentally. These limitations clearly indicate the urgency for systematic laboratory studies to identify the reaction products of neutral–neutral encounters relevant to interstellar gas-phase chemistry.

What experimental technique is suitable to investigate these gas-phase reactions? First, experiments must be performed under single-collision conditions. This means that, in a binary reaction A + BC → [ABC]* → AB + C, one species A reacts only with one species BC without collisional stabilization or successive reaction of the initially formed [ABC]* complex (exclusion of three-body reactions). This requirement guarantees that the nascent reaction product undergoes no secondary reaction. Secondly, highly unstable and reactive radicals, often with unknown spectroscopic properties, have to be probed. Hence, the majority of interesting interstellar radicals such as long-chain carbon chains, cummulenes, and sulfur-containing species cannot be sampled *via* optical detection schemes such as laser-induced fluorescence (LIF) and resonance-enhanced multi-photon ionization (REMPI), and a 'universal' detector is crucial. Finally, we have to take into consideration that a great variety of structural isomers can contribute to the reaction product (for example, the simple formula C_4H_5 has 25 local minima). Here, the knowledge of detailed chemical dynamics of a reaction can be employed to elucidate the product isomer(s).

In our experiments, all these requirements are fulfilled using the crossed molecular beams technique with a universal mass spectrometric detector,[20] *cf.* Section 2 for a detailed description. This set-up represents a versatile tool to (a) study reaction products under single-collision conditions without three-body reactions; (b) investigate the chemical dynamics of neutral–neutral reactions and (c) identify distinct structural isomers relevant to interstellar chemistry under well defined collision energies. To allow for an explicit assignment of reaction mechanisms and products, it is often crucial to combine

crossed molecular beams experiments with high level *ab initio* calculations for structure and energetics of possible intermediate collision complexes as well as reaction energies.[21] Recently, we initiated these experiments in our laboratory, elucidating the chemical dynamics and reaction products of exothermic atom–molecule and atom–radical reactions of $C(^3P_j)$ with acetylene, C_2H_2, ethylene, C_2H_4, methylacetylene, CH_3CCH, propylene, C_3H_6, and the propargyl radical, C_3H_3. These investigations provided collision-energy dependent (8.8–45.0 kJ mol^{-1}), doubly differential cross-sections to interstellar linear/cyclic tricarbon hydride[22] [l/c-C_3H ($^2\Pi_{1/2}$/$^2B_2$), reaction (1)], and to hitherto unobserved interstellar propargyl[23] [$C_3H_3(^2B_2)$, reaction (2)], butatrienyl[24] [n-$C_4H_3(^2A')$, reaction (3)], methylpropargyl [$C_4H_5(^2B_2$/$^2A'')$, reaction (4)] and diacetylene[26] [$C_4H_2(^1\Sigma_g^+)$, reaction (5)]:

$$C(^3P_j) + C_2H_2(^1\Sigma_g^+) \rightarrow \text{l-}C_3H(^2\Pi_{1/2}) + H(^2S_{1/2}), \tag{1}$$

$$\rightarrow \text{c-}C_3H(^2B_2) + H(^2S_{1/2}),$$

$$C(^3P_j) + C_2H_4(^1A_g) \rightarrow C_3H_3(^2B_2) + H(^2S_{1/2}), \tag{2}$$

$$C(^3P_j) + CH_3CCH(^1A_1) \rightarrow \text{n-}C_4H_3(^2A') + H(^2S_{1/2}), \tag{3}$$

$$C(^3P_j) + C_3H_6(^1A') \rightarrow C_4H_5(^2B_2/^2A'') + H(^2S_{1/2}), \tag{4}$$

$$C(^3P_j) + C_3H_3(^2B_2) \rightarrow C_4H_2(^1\Sigma_g^+) + H(^2S_{1/2}) \tag{5}$$

The identification of this carbon–hydrogen exchange under single-collision conditions demonstrated the importance of a one-step pathway to form free hydrocarbon radicals and closed-shell hydrocarbons through entrance-barrier-free reactions in interstellar environments. Further, the cyclic and linear C_3H isomers have both been identified around the dark molecular cloud TMC-1 and the carbon star IRC + 10216. In dark clouds, typical ratios of the cyclic *versus* the linear isomer are near unity, but decrease to 0.2 ± 0.1 around the carbon star. In particular, the circumstellar shell of IRC + 10216 contains a C_2H_2 as well as a $C(^3P_j)$ reservoir,[27] and formation of C_3H *via* neutral–neutral reaction very likely takes place. A common acetylene precursor to interstellar c/l-C_3H radicals *via* atom–neutral reaction with $C(^3P_j)$ can explain these astronomically observed isomer ratios.[28]

The present paper extends these crossed molecular beams investigations and presents results on the reactions of atomic carbon with hydrogen sulfide (H_2S), allene (H_2CCCH_2), vinyl radical (C_2H_3), and deuteroacetylene, C_2HD. Supplementary *ab initio* calculations were performed. Here, the reaction of carbon atoms with the closed-shell, sulfur-containing molecule, hydrogen sulfide, is the simplest organosulfur reaction to form carbon–sulfur-containing molecules and radicals in the interstellar medium. The second experiment investigates the chemical dynamics and products of the reaction of ground-state atomic carbon with allene and compares these findings with reaction (3) studied recently in our laboratory. These studies allow an explicit identification of the product isomer and outline the necessity to include distinct reactant as well as product isomers in chemical reaction networks modelling the chemistry in interstellar environments. Further, we investigated the reaction of atomic carbon with the vinyl radical to study the formation of interstellar C_3H_2 isomers *via* C_3H_3 reactive intermediates. Finally, the reaction of $C(^3P_j)$ with C_2HD is closely related to reaction (1) and allows us to investigate the deuterium isotope effect on the formation of interstellar l/c-C_3D.

2   Experimental

The reactive scattering experiments are carried out in a universal crossed molecular beam apparatus described in detail in ref. 29. Fig. 1 shows a schematic top view of the
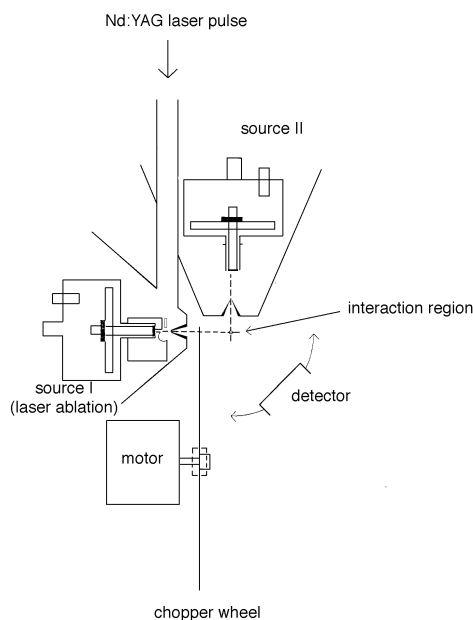
Fig. 1 Schematic top view of the crossed molecular beams set-up

set-up. The 35″ crossed molecular beams machine consists of two source chambers (10^{-4} mbar), a stainless-steel scattering chamber (10^{-7} mbar), and a rotatable, differentially pumped quadrupole mass spectrometric detector (10^{-11} mbar). The supersonic carbon beam is generated in the primary source *via* laser ablation of graphite.[30] Here, the 30 Hz, 30–65 mJ, 266 nm output of a Spectra Physics GCR-270-30 Nd : YAG laser is focused on a rotating carbon rod. Ablated carbon atoms in their ^3P_j electronic ground state are seeded into neon or helium gas released by a Proch–Trickl pulsed valve.[31] A four-slot chopper wheel is mounted 40 mm after the ablation zone to select a 9.0 μs segment of the seeded carbon beam. This segment crosses a second, pulsed reactant beam under a well defined collision energy at 90° under single collision conditions in the interaction region of the scattering chamber. Neat and seeded mixtures of H_2S, H_2CCCH_2, and C_2HD are held at 1 atm backing pressure. C_2H_3 was generated by 193 nm photolyses of 10% C_2H_3Br precursor seeded in helium carrier gas.

Reactively scattered species are monitored using a differentially pumped quadrupole mass spectrometer, rotatable in the plane of the beams with respect to the interaction region. Differentially pumped regions I and II reduce the gas load from the main chamber, whereas region III contains the Brink-type electron impact ionizer,[32] surrounded by a liquid-nitrogen cold shield, the quadrupole mass filter, and the Daly-type scintillation particle detector.[33] Despite this differential pumping set-up, molecules desorbed from wall surfaces lying on a straight line with the electron impact ionizer (straight-through-molecules) cannot be avoided, since the mean free path of these species is of the order of 10^3 m compared to maximum detector dimensions of *ca.* 1 m. To reduce these straight-through-molecules, a copper plate is attached to a two-stage closed cycle helium refrigerator and cooled to *ca.* 10 K. Since the copper shield is located between the two skimmers and the scattering region, the ionizer 'views' a cooled surface from which only H_2 and He desorb at 10 K.

The velocity distribution of the products is determined recording the time-of-flight (TOF) spectra at different laboratory angles Θ between $-25°$ and $75°$ with respect to

the carbon beam. In this TOF mode, the mass spectrometric controller is set at a constant mass to charge ratio (m/z) and records the time-dependent number density of reactively scattered species at this m/z value at a constant laboratory angle Θ, $I(\Theta, t)$. If we integrate the TOF spectra at different laboratory angles, we obtain the intensity distribution in the laboratory reference frame (LAB).

3 Data analysis

In the previous section we described the crossed molecular beams set-up. Now, we present our method of analysis of the laboratory data. For the physical interpretation of the reactive scattering data, it is necessary to transform the laboratory data into the center-of-mass (CM) system, *cf* Fig. 2. An observer in the laboratory frame notices that the CM moves with velocity $v(CM)$. However, if this observer dwells at the CM, the CM is at rest. Fig. 2 shows the relation between both reference frames. In the experiment, a beam of species A with a laboratory velocity $v(A)$ crosses a beam of species BC with a laboratory velocity $v(BC)$ at 90° giving the relative velocity of A with respect to BC

$$\mathbf{g} = v(A) - v(BC) \tag{I}$$

In the laboratory system, the CM frame moves with velocity $v(CM)$ calculated with the masses of the reactants $m(A)$ and $m(BC)$

$$v(CM) = m(A)v(A) + m(BC)v(BC)]/[m(A) + m(BC)] \tag{II}$$

The CM velocity vector divides **g** into two parts, the velocity of A and BC in the CM frame, **u**(A) and **u**(BC), respectively. The magnitude of these vectors is inversly proportional to the mass ratio of the reactants. To convert the laboratory data to the CM system, we use a forward-convolution routine to fit the TOF spectra $I(\Theta, t)$ at different laboratory angles Θ and the product angular distribution in the laboratory frame (LAB).[34,35] This procedure initially guesses the angular flux distribution $T(\theta)$ and the translational energy flux distribution $P(E_T)$ in the CM frame. Here, θ defines the scattering angle in the CM system measured from the A beam and E_T the CM translational energy. Then, TOF spectra and LAB distribution were calculated from these $T(\theta)$ and $P(E_T)$ accounting for the velocity and angular spread of both beams, the detector acceptance angle, and the ionizer length. Both $T(\theta)$ and $P(E_T)$ are refined iteratively until a reasonable fit of the experimental data is achieved.
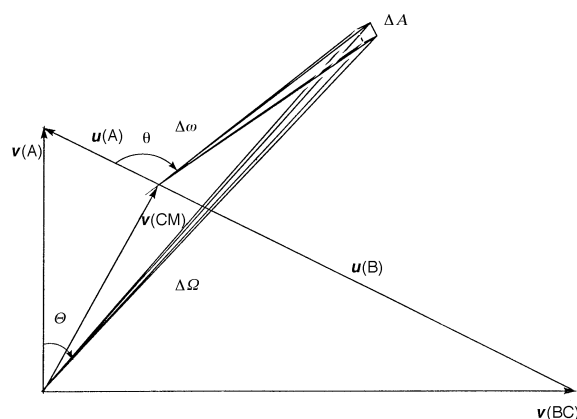

Fig. 2 Relation between the LAB and CM reference frames

In detail, four transformation steps are necessary. First, we transform the $I(\Theta, t)$ time domain to the velocity domain recalling that

$$I(\Theta, t)\,\mathrm{d}t = I(\Theta, v)\,\mathrm{d}v \qquad (III)$$

and

$$\frac{\mathrm{d}v}{\mathrm{d}t} = -\frac{v^2}{L} \qquad (IV)$$

with the velocity v and ionizer length L. Putting eqn. (IV) into (III) gives

$$I(\Theta, t) = -I(\Theta, v)v^2/L \qquad (V)$$

Secondly, the detector analyses number density, whereas $T(\theta)$ and $P(E_T)$ represent flux distributions. Hence, we have to transform a number density distribution (molecules cm^{-3}) to a flux distribution (molecules cm^{-1} s^{-1}). Here, the product of $I(\Theta, v)v$ is nothing else but a flux distribution in the laboratory frame defined as $\sigma(\Theta, v)$, yielding:

$$I(\Theta, t) = -\sigma(\Theta, v)v/L \qquad (VI)$$

Thirdly, we have to transform $\sigma(\Theta, v)$ to the CM flux distribution $\sigma(\theta, u)$ with the velocity u of the product. The v^2/u^2-transformation Jacobian can be derived by considering the cross-section proportional flux per unit time in a solid angle to be constant in the laboratory and CM frames:

$$\sigma(\Theta, v)\,\Delta\Omega = \sigma(\theta, u)\,\Delta\omega \qquad (VII)$$

where $\Delta\Omega$ is the solid angle sustained by the detector aperture ΔA in the laboratory, and the solid angle $\Delta\omega$ in the CM frame. Recalling the definition of a solid angle, *i.e.* $\mathrm{d}\Omega = \mathrm{d}A/r^2$ with the defining aperture of area $\mathrm{d}A$ at a distance r from the interaction region and $\Delta\Omega = \Delta A/(vt)^2$ and $\Delta\omega = \Delta A/(ut)^2$, we put these equations into eqn. (VII) to obtain the transformation Jacobian. Now, we can modify eqn. (VI) to

$$I(\Theta, t) = -\sigma(\theta, u)v^3/L/u^2 \qquad (VIII)$$

The fourth step transforms the velocity distribution to the translational energy distribution using energy and momentum conservation, with $\bar{\mu} = m_{AB}(m_{AB}/m_{AB}/m_C + 1)$ and the masses of the products AB and C, to give

$$\sigma(\theta, u) = \sigma(\theta, E_T)\bar{\mu}u \qquad (IX)$$

yielding

$$I(\Theta, t) = -\sigma(\theta, E_T)\bar{\mu}v^3/L/u \qquad (X)$$

Here, $\sigma(\theta, E_T)$ is the double differential cross-section in the CM reference frame. $\sigma(\theta, E_T)$ is proportional to $T(\theta)$ and $P(E_T)$, hence

$$\sigma(\theta, E_T) = C \times T(\theta)P(E_T) \qquad (XI)$$

with a constant, C. Since $T(\theta)$ and $P(E_T)$ are normalized, C is obtained by integrating $\sigma(\theta, E_T)$ over θ, φ (the angle around the relative velocity vector g), and E_T:

$$\sigma(E) = \int_0^\infty \int_0^{2\pi} \int_0^\pi P(E_T)T(\theta)\sin\theta\,\mathrm{d}\theta\,\mathrm{d}\varphi\,\mathrm{d}E_T = C \qquad (XII)$$

This identifies the constant C as the integrated reaction cross-section of the bimolecular reaction A + BC → AB + C at a collision energy E. Hence, the final relation between the TOF spectra at a laboratory angle Θ, $I(\Theta, t)$, and the iteratively refined CM flux distributions $T(\theta)$ and $P(E_T)$ with the constant C is given by

$$I(\Theta, t) = C\,T(\theta)P(E_T)v^3/u \qquad (XIII)$$

4 Results and Discussion

4.1 $C(^3P_j) + H_2S$

The crossed beams experiments were performed at two different collision energies of 16.7 and 42.4 kJ mol^{-1}. Fig. 3 and 4 show the laboratory angular distributions as well as TOF spectra of the reactive scattering signal at $m/z = 45$ (HCS/HSC) at a selected collision energy of 42.4 kJ mol^{-1}. TOF spectra at $m/z = 44$ show the identical shapes as $m/z = 45$, indicating that HCS$^+$ fragments partly to CS$^+$ in the electron impact ionizer and that no CS is formed in our experiments. Further, no radiative association to any H$_2$CS isomer was observed at $m/z = 46$.
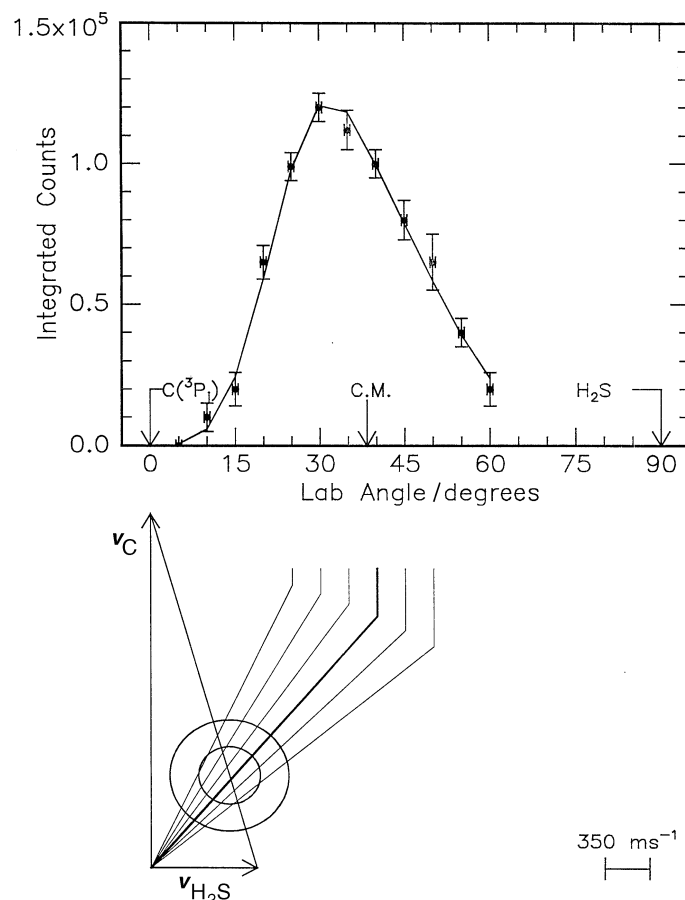
Fig. 3 Top: HCS product laboratory angular distribution of the reaction $C(^3P_j) + H_2S(^1A_1)$ at a collision energy 42.4 kJ mol^{-1}. Filled circles and 1σ error bars indicate experimental data, the solid lines the calculated distribution, and C.M. the CM angle. Bottom: Corresponding velocity vector diagram. v_C and v_{H_2S} indicate the velocities of the carbon and hydrogen sulfide beam in the LAB frame. The inner circle stands for the maximum CM recoil velocity of the HSC isomer, the outer circle for the HCS in the CM frame, assuming all available energy channels into translational energy of the products. The solid lines point to distinct laboratory angles whose TOFs are shown in Fig. 4.
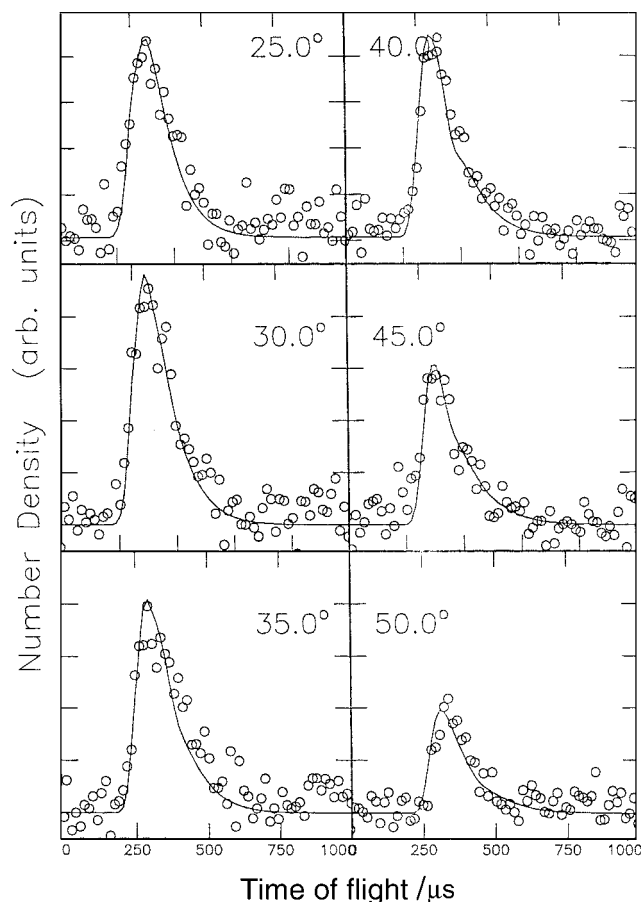
Fig. 4 Normalized TOF data of HCS at $m/z = 45$ at a collision energy of 42.4 kJ mol^{-1}. ($\bigcirc$) Experimental data, (———) the fit.

Now we investigate the chemical dynamics of the reaction to unravel the intermediate H_2CS complex(es) as well as product HCS isomer(s). The experimentally found high-energy cut-offs of 208 and 232 kJ mol^{-1} agree very well with the sum of recent *ab initio* reaction energy for the HCS isomer[36] and the relative collision energies, *i.e.* 201 and 226 kJ mol^{-1}. The less stable HSC isomer is expected to show cut-offs at 35.0 and 60.7 kJ mol^{-1} and, hence, can be excluded as a major contribution to our reactive scattering signal. The shape of the CM angular distributions (Fig. 5) depends strongly on the collision energy E_c. As E_c is increased, $T(\theta)$ changes from an isotropic, forward–backward symmetric to a more forward scattered distribution. This finding suggests only one reaction channel following indirect reactive scattering dynamics through a complex formation. At lower collision energy, the fragmenting H_2CS isomer has a lifetime longer than its rotational period, but as the collision energy rises to 42.4 kJ mol^{-1} [37] the lifetime of the complex is reduced to less than one rotational period.

The identification of the HCS product clearly excludes decomposing singlet or triplet H_2SC **1/2**, *cf.* Fig. 6, since an S—H bond rupture would yield solely the HSC isomer. Further, the experimentally found $T(\theta)$ shows a forward peaking with respect to the carbon beam higher collision energy. This requires that the incorporated carbon atom
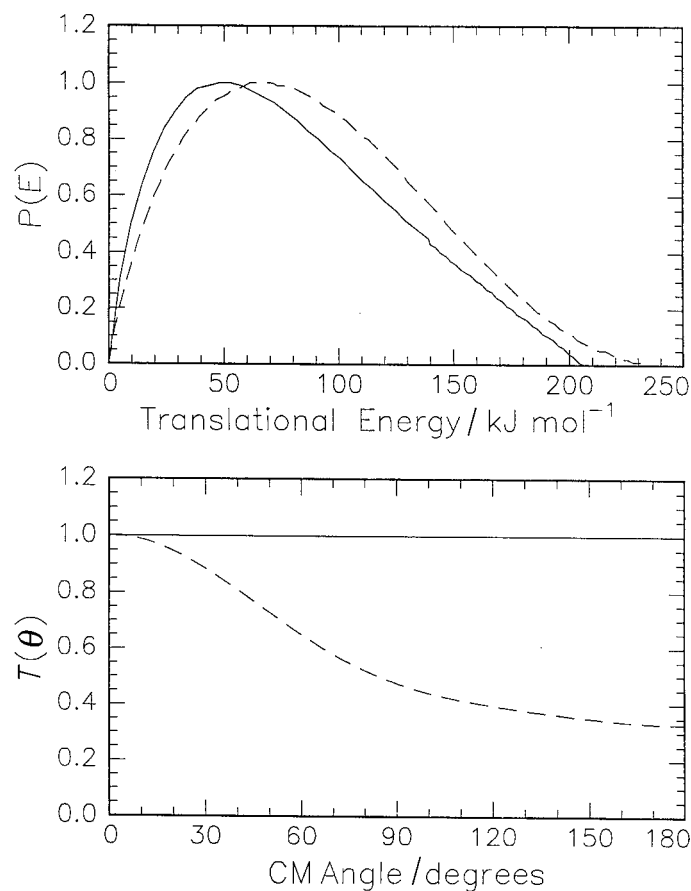
Fig. 5 CM angular flux distributions (bottom) and translational energy flux distributions (top) for the reaction $C(^3P_j) + H_2S(X^1A_1)$ at peak collision energies of 16.7 (——) and 42.4 kJ mol^{-1} (– – –)

and the leaving H atom must be located on opposite sites of the rotational axes. Based on the calculated *ab initio* geometries of triplet and singlet H_2CS **6/7**, no rotation axis fulfills this requirement. Hence, thioformaldehyde can also be excluded as the decomposing complex. Based on these conclusions, thiohydroxycarbenes **3**, **4**, and **5** are the only remaining intermediates. Each of these complexes can rotate around the B/C axis to account for the forward peaked CM angular distribution, yielding HCS and H in the final bond rupture. The dynamics leading to the thiohydroxycarbene itself are governed by an addition of $C(^3P_j)$ to H_2S to form triplet 2,2-dihydrothiocarbonyl **2**. A direct insertion into the S—H bond of H_2S to yield triplet thiohydroxycarbene, **3** can likely be ruled out considering the symmetry-forbidden nature. Therefore, one expects a significant entrance barrier, much larger than our lowest collision energy. Owing to the heavy sulfur atom and the narrow singlet–triplet gap of **1** and **2** intersystem crossing (ISC) to **1** might occur followed by an H migration to **4/5**. Alternatively, **2** could undergo H migration to **3** and subsequent ISC to **4/5**.

4.2 $C(^3P_j) + H_2CCCH_2$

The reactive scattering experiments were performed at two collision energies of 19.6 and 39.3 kJ mol^{-1}. In strong analogy to reactions (1)–(5), the carbon–hydrogen exchange
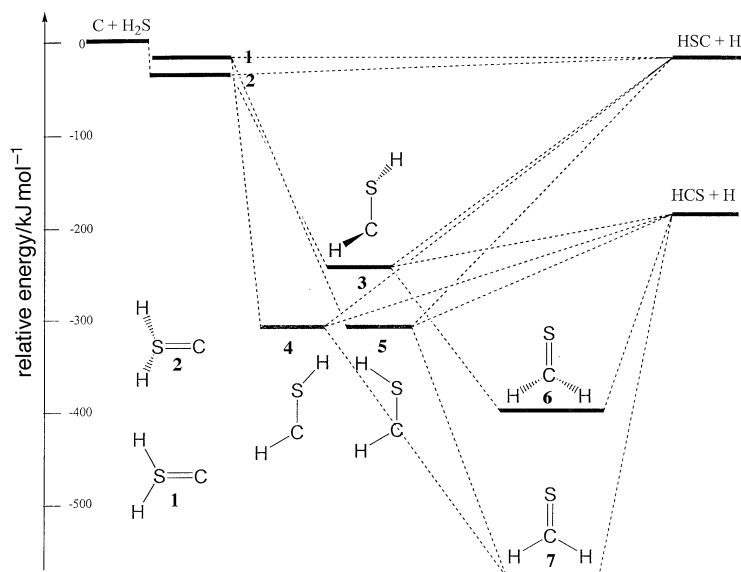
Fig. 6 Schematic energy level diagram of the $C(^3P_j) + H_2S(X^1A_1)$ reaction and *ab initio* structures of calculated H_2CS and HCS isomers

channel also dominates the product distributions, *cf.* Fig. 7 and 8. The reactive scattering signal is only observed at $m/z = 51$, *i.e.* C_4H_3. TOF spectra were recorded at lower m/z values, 50–48, but show identical patterns. This finding indicates that the signal at these m/z ratios originates from cracking of the parent in the ionizer. In addition, no radiative associations to C_4H_4 ($m/z = 52$) could be detected. This result demonstrates that no internally excited C_4H_4 collision complex survives under single-collision conditions in our experiments as well as in the ISM.

Best fits of TOF spectra and LAB distributions are achieved with $P(E_T)$s extending to maximum translational energies of $E_{max} = 215$ kJ mol^{-1} and 240 kJ mol^{-1} at our lower and higher collision energy, respectively (Fig. 9). This high-energy cut-off can be employed to identify the product isomers if their energetics are well separated. Within the error limits, data are consistent with the formation of n-C_4H_3 at both collision energies, since the high-energy cut-offs are expected at 213.6 kJ mol^{-1} at lower and 233.3 kJ mol^{-1} at higher collision energy.

At lower collision energy, the $T(\theta)$ is symmetric around $\pi/2$. As the collision energy rises, the $T(\theta)$ shape changes to a more forward scattered distribution, *i.e.* increasing intensity at 0°. In strong analogy to the reaction of $C(^3P_j)$ with H_2S, these findings suggest a reduced lifetime of the decomposing C_4H_4 complex as the collision energy rises. Complex formation takes place, but the well-depth along the reaction coordinate is too shallow to allow multiple rotations, and the complex decomposes with a random lifetime distribution before one full rotation elapses.

We now investigate the chemical dynamics of the reaction. The identification of the n-C_4H_3 isomer strongly suggests that $C(^3P_j)$ attacks the π-bond in allene to form a substituted triplet cyclopropylidene intermediate **1**, *cf.* Fig. 10, rotating in the molecular plane which contains the four carbon atoms. **1** undergoes a subsequent ring opening to triplet butatrienylidene **2** followed by a C—H bond rupture to yield atomic hydrogen and n-C_4H_3 or a hydrogen shift to methylpropargylene **3** prior to decomposition of **3** to n-C_4H_3 + H. To distinguish between these two possibilities, we re-ran the crossed
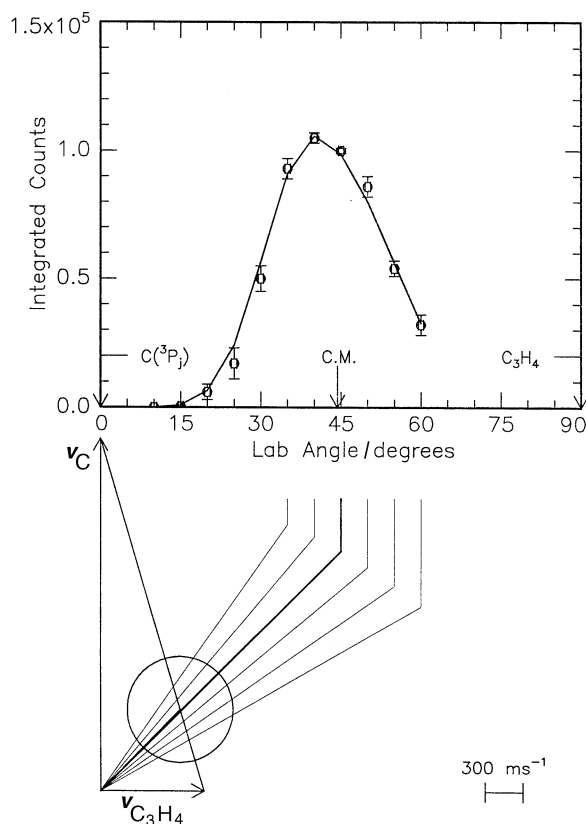
Fig. 7 Top: C_4H_3 product LAB angular distribution of the reaction $C(^3P_j) + H_2CCCH_2$ at a collision energy 39.3 kJ mol^{-1}. Filled circles and 1σ error bars indicate experimental data, the solid lines the calculated distribution, and C.M. the CM angle. Bottom: Corresponding velocity vector diagram. v_C and $v_{C_3H_4}$ indicate the velocities of the carbon and allene beam in the LAB frame. The circle stands for the maximum CM recoil velocity of the n-C_4H_3 isomer, assuming all available energy channels into translational energy of the products. The solid lines point to distinct laboratory angles whose TOFs are shown in Fig. 8.

molecular beams experiments of $C(^3P_j)$ with methylacetylene at the same collision energies as those obtained with allene. Our data show that, at all angles, the ratio of the intensity of the integrated TOFs at $m/z = 51$, 50, and 49 is identical at the higher collision energy for both $C(^3P_j)$ + allene and methylacetylene reactions, *i.e.* 0.3 ($m/z = 51$) : 1.0 ($m/z = 50$) : 0.5 ($m/z = 49$). Both LAB distributions are also identical. These data strongly indicate that, at higher collision energy, the decomposing C_4H_4 complex and the reaction intermediate are the same in both reactions. Since triplet methylpropargylene was assigned as the decomposing complex in reaction (2), we conclude that the chemical dynamics of allene reacting with $C(^3P_j)$ are initiated by an attack to the alkenic π-bond to form a triplet cyclopropylidene derivative, followed by a ring opening to **2**, a H atom migration to **3** and final C—H bond rupture to the n-C_4H_3 isomer. However, at lower collision energy, ratios of $m/z = 51$ to 50 to 49 of both the methylacetylene and allene reaction with atomic carbon do not match. Hence, we must conclude that their chemical dynamics are different. We pointed out earlier, that a second isomer might contribute to the reactive scattering signal of the reaction C/CH_3CCH at $m/z = 51$.[24] A detailed analysis shows that a second, cyclic C_4H_3 isomer **4**, **5** or **6** is formed as well as at lower collision energy n-C_4H_3.[38]
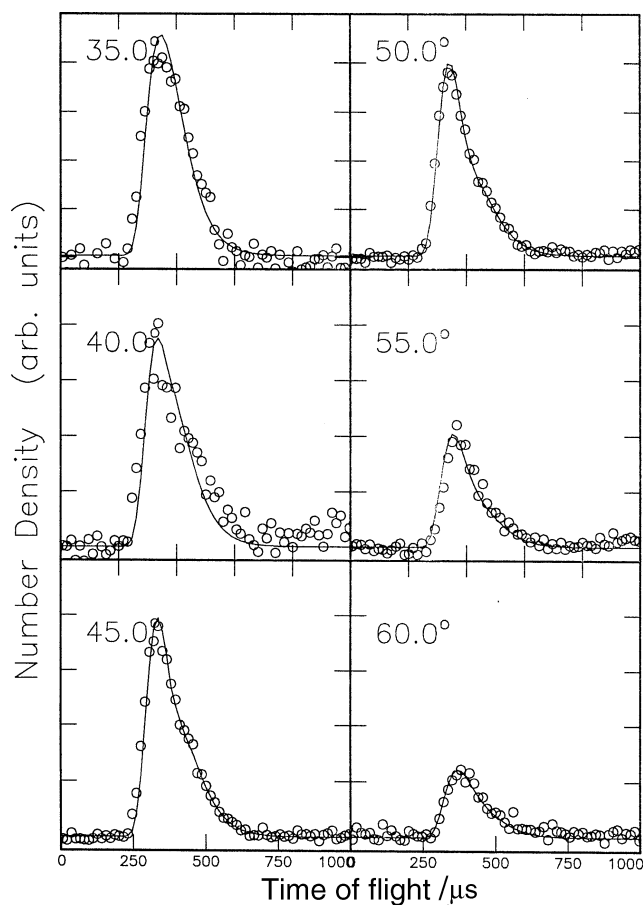
Fig. 8 Normalized TOF data of C_4H_3 at $m/z = 51$ at a collision energy of 39.3 kJ mol^{-1}.
(○) Experimental data, (——) the fit.

4.3 $C(^3P_j) + C_2H_3$

A reactive scattering signal was only observed at $m/z = 38$, *i.e.* C_3H_2. Owing to the limited signal-to-noise ratio and the necessary background subtraction procedure, we can present only one TOF recorded at the CM angle of 53°, Fig. 11. One must keep in mind that it took *ca.* 9 months to modify and optimize the crossed molecular beams machine for this two-laser experiment, to maximize the number density in the C_2H_3 beam to obtain this reactive scattering signal. Currently, the crossed molecular beam machine is undergoing a major refit to an oil-free operation. This will reduce the background and enhance the signal-to-noise level, thus reducing the data accumulation time by a factor of *ca.* 10. With these experimental improvements, this experiment will continue in the near future.

Although we have not yet been able to record a full angular distribution, the identification of C_3H_2 under single-collision conditions underlines the potential importance of this reaction to form C_3H_2 isomers in the ISM. Hence, at this stage we can only outline all feasible reaction pathways without resolving the actual one(s), *cf.* Fig. 12. Atomic carbon can attack the alkenic π bond to yield a cyclic C_3H_3 isomer **1**. Depending on its lifetime and the chemical reaction dynamics, **1** undergoes C—H bond cleavage to form singlet/triplet C_3H_2 **2** and/or ring opens to the propargyl radical **3**. **3** either loses an H
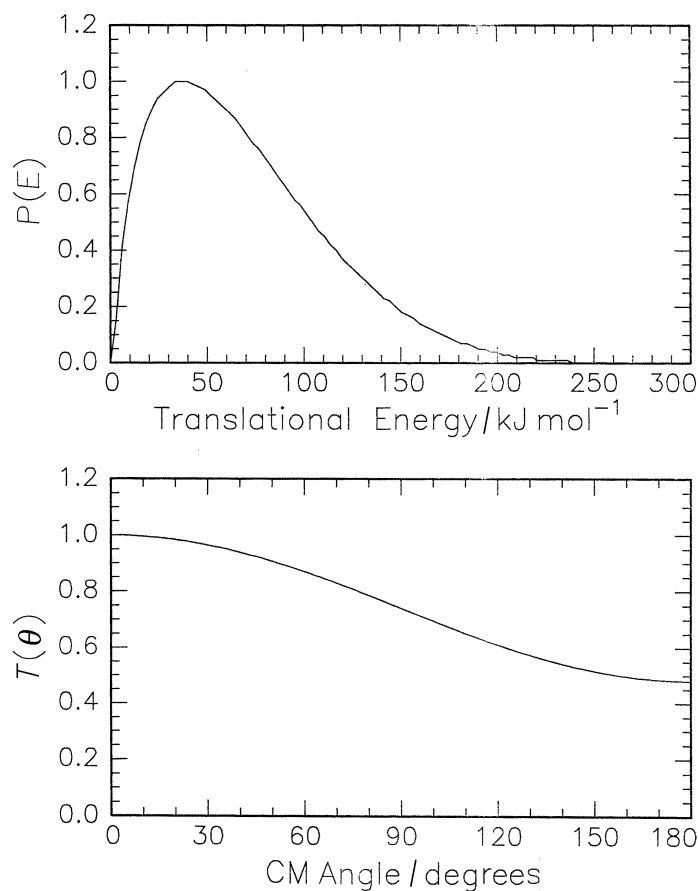
Fig. 9 CM angular flux distribution (bottom) and translational energy flux distribution (top) for the reaction $C(^3P_j) + H_2CCCH_2$ at a selected energy of 39.3 kJ mol^{-1}

atom at the acetylenic carbon atom to form singlet/triplet vinylidenecarbene, H_2CCC **4**, or at the alkenic carbon atom to yield triplet/singlet propargylene **5**. Based on the energetics, all three isomers can be formed in either the singlet or triplet state; the nature of the C_3H_2 isomer(s) formed remains to be resolved.
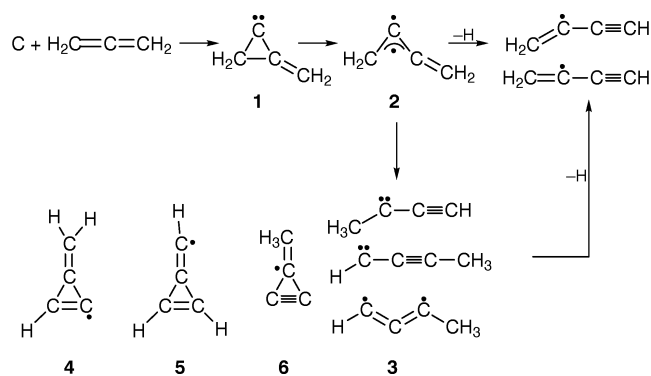
Fig. 10 Simplified scheme of the $C(^3P_j) + H_2CCCH_2$ reaction. The equilibrium structures of **3** and *n*-C_4H_3 are under investigation.[53]
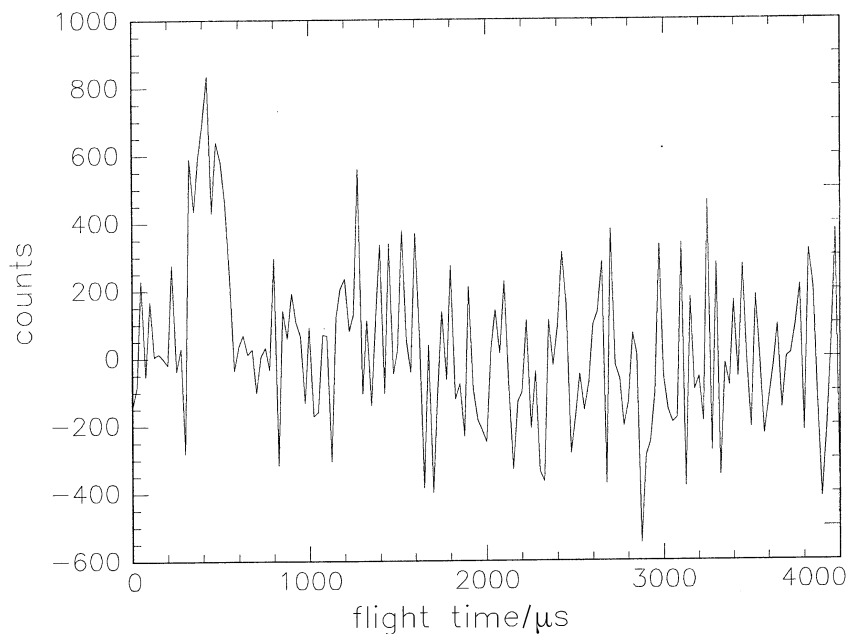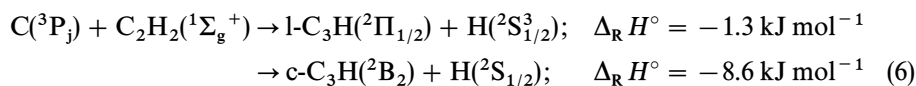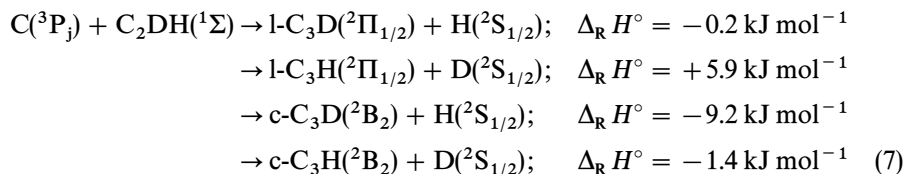
Fig. 11 TOF spectra of C_3H_2 at $m/z = 38$ at the CM angle of $53°$

4.4 C(^{3}P$_j$) + C$_2$HD

Our *ab initio* calculations show that the isotopic substitution of H *versus* D shows a profound effect on the energetics of the title reaction.[39] Earlier investigations revealed that formation of both the c-C_3H and l-C_3H isomers are exothermic by 8.6 and 1.3 kJ mol^{-1}, respectively:

$$C(^3P_j) + C_2H_2(^1\Sigma_g^+) \rightarrow l\text{-}C_3H(^2\Pi_{1/2}) + H(^2S_{1/2}^3); \quad \Delta_R H° = -1.3 \text{ kJ mol}^{-1}$$
$$\rightarrow c\text{-}C_3H(^2B_2) + H(^2S_{1/2}); \quad \Delta_R H° = -8.6 \text{ kJ mol}^{-1} \quad (6)$$

Substituting one H atom by D gives the following reaction energies:

$$C(^3P_j) + C_2DH(^1\Sigma) \rightarrow l\text{-}C_3D(^2\Pi_{1/2}) + H(^2S_{1/2}); \quad \Delta_R H° = -0.2 \text{ kJ mol}^{-1}$$
$$\rightarrow l\text{-}C_3H(^2\Pi_{1/2}) + D(^2S_{1/2}); \quad \Delta_R H° = +5.9 \text{ kJ mol}^{-1}$$
$$\rightarrow c\text{-}C_3D(^2B_2) + H(^2S_{1/2}); \quad \Delta_R H° = -9.2 \text{ kJ mol}^{-1}$$
$$\rightarrow c\text{-}C_3H(^2B_2) + D(^2S_{1/2}); \quad \Delta_R H° = -1.4 \text{ kJ mol}^{-1} \quad (7)$$

Crossed molecular beams experiments are underway.
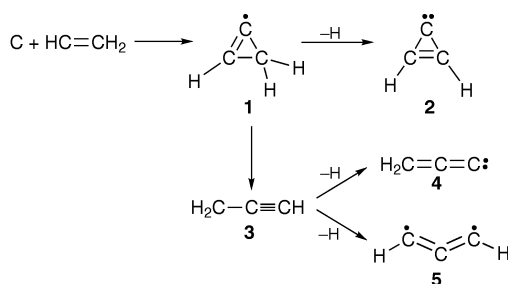

Fig. 12 Schematic pathways to distinct C_3H_2 isomers *via* C_3H_3 intermediates

5 Astrophysical implications

5.1 $C(^3P_j) + H_2S$

The $C(^3P_j)$–H_2S system represents the prototype reaction of ubiquitous interstellar carbon atoms with the simplest saturated sulfur molecule, hydrogen sulfide, to synthesize sulfur-containing species *via* a single atom–neutral collision. The insights in the chemical dynamics of this reaction reveal an important pathway to hitherto astronomically unobserved HCS. The thermodynamically less stable HSC isomer could not be detected in our experiments, and upper limits show a maximum contribution of 10% to the reactive scattering signal. Further, this reaction does not form CS through H_2 elimination. H_2S is ubiquitous in the ISM and has been observed, for example, in molecular clouds TMC-1 and OMC-1 toward the star-forming region SgrB2, and around the circumstellar envelope of the carbon star IRC+10216.[40,41] Upon reaction of $C(^3P_j)$ with hydrogen sulfide, the very first C—S bond is formed. HCS could react with $C(^3P_j)$ to form the astronomically observed C_2S:[42]

$$C(^3P_j) + H_2S \rightarrow HCS + H \tag{8}$$

$$C(^3P_j) + HCS \rightarrow C_2S + H \tag{9}$$
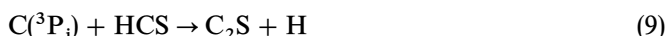
Very recently, experimental as well as theoretical rotational constants of the HCS radical have been obtained.[43] These will be applied to search for the HCS radical in the ISM.
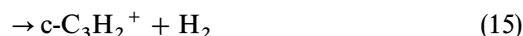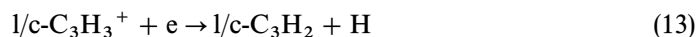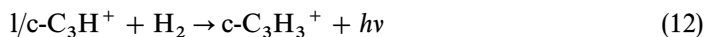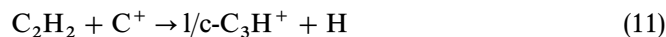
5.2 $C(^3P_j) + H_2CCCH_2$

Methylacetylene, CH_3CCH, has been widely observed in dark, molecular clouds such as OMC-1 and TMC-1 in high fractional abundances between $(4–6) \times 10^{-9}$ cm^{-3} by microwave spectroscopy.[44] A second C_3H_4 isomer, allene (H_2CCCH_2), holds no permanent electric dipole moment and, hence, shows no rotational spectrum. Although H_2CCCH_2 should be detectable *via* IR spectroscopy in the circumstellar shell of, *e.g.* the carbon star IRC+10216, this isomer has escaped any astronomical identification so far. Despite this failure, the allene isomer is strongly expected to be present in dark, molecular clouds as well as in the outflow of carbon stars and, hence, was included in chemical reaction networks modelling time-dependent chemistry in these extraterrestrial environments[16] and in astrochemical databases.[45] However, owing to insufficient laboratory data, these models cannot predict the formation of distinct structural isomers and, hence, are unable to account for different chemical reactivities of allene *versus* methylacetylene. Therefore, the explicit identification of the n-C_4H_3 isomer, as well as a second, cyclic isomer in the reaction of $C(^3P_j)$ with methylacetylene, outline the necessity to include distinct reactant as well as product isomers in chemical reaction network modelling of the chemistry in interstellar environments.

5.3 $C(^3P_j) + C_2H_3$

Singlet cyclopropenylidene, hereafter referred to as c-C_3H_2, was detected in 1985 *via* microwave spectroscopy in the ISM.[46] Subsequent quantitative surveys indicated that c-C_3H_2 is one of the most abundant molecules in interstellar environments such as dark clouds TMC-1, Oph A, Ori A, and SgrB2 and the carbon star IRC+10216, holding fractional abundances up to 10^{-8} molecules cm^{-3}.[47] In diffuse clouds, cyclopropenylidene is depleted by a factor of *ca.* 100.[48] A second C_3H_2 isomer, singlet vinylidenecarbene, H_2CCC, was discovered six years later by Cernicharo *et al.* towards TMC-1.[49] Compared with cyclopropenylidene, its fractional abundance is only 1–2%.

Most surprisingly, however, a third isomer triplet propargylene, although more stable than vinylidenecarbene, has never been observed in the ISM.

However, despite high number densities of c-C_3H_2, the formation mechanism of this cyclic molecule has never been resolved either experimentally or theoretically. Typical ion–molecule reaction networks postulate elaborate, multiple ion–molecule reactions:[50]

$$C + \text{cosmic ray} \rightarrow C^+ + e \tag{10}$$

$$C_2H_2 + C^+ \rightarrow l/c\text{-}C_3H^+ + H \tag{11}$$

$$l/c\text{-}C_3H^+ + H_2 \rightarrow c\text{-}C_3H_3{}^+ + h\nu \tag{12}$$

$$l/c\text{-}C_3H_3{}^+ + e \rightarrow l/c\text{-}C_3H_2 + H \tag{13}$$

$$C_2H_4 + C^+ \rightarrow c\text{-}C_3H_3{}^+ + H \tag{14}$$

$$\rightarrow c\text{-}C_3H_2{}^+ + H_2 \tag{15}$$

$$\rightarrow l\text{-}C_3H_2{}^+ + H_2 \tag{16}$$

$$l/c\text{-}C_3H_3{}^+ + e \rightarrow l/c\text{-}C_3H_2 + H \tag{17}$$

These approaches, however, neither reproduced fractional abundances, isomer-ratios of C-C_3H_2 *vs.* H_2CCC, nor accounted for high deuterium enrichment observed in c-C_3HD *vs.* c-C_3H_2, *i.e.* an observed value of 0.08 in TMC-1 *vs.* 0.015 obtained in chemical models. Hence, the reaction of atomic carbon with the vinyl radical can replace the ion–molecule based four- to five-step synthesis through a single reactive encounter to form C_3H_2 isomers.

5.4 C(^3P_j) + C$_2$HD

The reaction of C(^3P_j) with C_2HD is closely related to reaction (1) and investigates the deuterium isotope effect on the formation of l/c-C_3D. Although the deuteriated isomers have never been observed in the ISM, Yamamoto *et al.* suggested that, at least, the c-C_3D radical should be present and be observable towards TMC-1 in the microwave region.[51] Recent crossed beam investigations combined with *ab initio* calculations of reaction (1) showed that the synthesis of c-C_3H is exothermic by 8.6 kJ mol^{-1}, compared with synthesis of the l-C_3H isomer that is exothermic by only 1.3 kJ mol^{-1}.[52] The substitution of one H atom by a D atom in acetylene changes the zero-point vibration energy and, hence, the reaction energy.

Based on our *ab initio* calculations, the formation of l-C_3H from C_2DH cannot be covered by the reactants' average translational energy of *ca.* 0.08 kJ mol^{-1} in cold molecular clouds, and only l-C_3D can be formed. Both reaction pathways to the cyclic isomer, however, are exothermic. These findings should be reflected in prospective astronomical surveys of the fractional abundances of l-C_3H *vs.* l-C_3D toward dark clouds. Our results strongly suggest enhanced deuterium enrichment in the linear isomer *versus* the cyclic one. In warmer interstellar environments, such as the outflow of carbon stars, the reaction endothermicity to l-C_3H of only 5.9 kJ mol^{-1} could be compensated by the enhanced averaged translational temperature of the reactants. Hence, compared with cold clouds, the isotopic enrichment is expected to be less pronounced.

6 Conclusions

The crossed molecular beams technique and *ab initio* calculations have been established as a universal and powerful tool to investigate neutral–neutral reactions of potential importance to interstellar chemistry under well defined reaction conditions. All C(^3P_j) reactions with unsaturated hydrocarbons and H_2S studied so far are barrier-less and are dominated by a carbon–hydrogen exchange channel. Based on the CM angular flux

distribution $T(\theta)$ and CM translational energy flux distribution, $P(E_T)$, the crossed molecular beams approach with a universal detector is able to distinguish between distinct hydrocarbon and thiohydrocarbon product isomers. This carbon–hydrogen exchange channel represents an alternative pathway to competing ion–molecule reactions. Further, it clearly underlines that not only are reaction rate constants important to model interstellar chemistry, but also that the inclusion of distinct structural isomers into these interstellar reaction networks is equally important. This versatile concept can be used further to predict the formation of these radicals in interstellar environments. If regions of high fractional abundances of atomic carbon overlapping with those of the second reactant radical/molecule are identified, then the reaction takes place in these environments. Since none of the species, except $l\text{-}C_3H/c\text{-}C_3H$, have been detected in the ISM, our results should encourage astronomical search for these hitherto unobserved radicals.

In addition, no radiative association takes place under single-collision conditions. If the reactions studied here take place on interstellar grains, the collision complexes involved could be stabilized. For example, the reaction of $C(^3P_j)$ with H_2S on interstellar grains might resolve the anticorrelation of H_2CS and H_2S in carbon-rich dark clouds TMC-1. Since H_2S is formed on interstellar grains, implanted carbon atoms from the gas phase very likely react to give a thiohydroxycarbene intermediate. Its lifetime is expected to be longer in a solid matrix as compared with our crossed beam experiments, and a second H-migration to thioformaldehyde might take place.

The work presented so far is just the first steps towards a better understanding of the importance of neutral–neutral reactions in contrast to ion–molecule reactions in the formation of molecules and radicals in extraterrestrial environments. The chemical dynamics of atom–radical and radical–radical reactions in the ISM are completely unknown. Both reaction classes, however, are expected to have a profound impact on chemistry in interstellar and hydrocarbon-rich planetary environments at very low temperatures, down to 10 K: reactive encounters between $C(^3P_j)$, CH, C_2H, and open-shell hydrocarbons such as CH, C_2H, C_2H_3 and C_3H_3 radicals are thought to resemble prototype reactions proceeding without any barrier in the entrance channel. Therefore, these reactions are strongly expected to form complex species, even in the coldest known interstellar clouds where the average kinetic energy of reactant molecules is *ca.* 0.08 kJ mol^{-1} and will be studied in the future. We will keep you informed.

References

1 *Interstellar Processes*, ed. D. J. Hollenbach and H. A. Thronson, Reidel, Dordrecht, 1987.
2 H. Scheffler and H. Elsässer, *Physics of the Galaxy and Interstellar Matter*, Springer, Berlin, 1988.
3 J. M. Greenberg, *Astron. Astrophys.*, 1971, **12**, 240; A. G. G. M. Tielens and L. J. Allamandola, in ref. 1, p. 397.
4 D. C. B. Whittet, in *Dust and Chemistry in Astronomy*, ed. T. J. Millar and D. A. Williams, Institute of Physics, Bristol, 1993, p. 1; B. Schmitt, in *Molecules and Grains in Space*, ed. I. Nenner, AIP Press, New York, 1994, p. 735; W. A. Schutte *et al.*, *Astron. Astrophys.*, 1996, **309**, 633; A. G. G. M. Tielens, L. J. Allamandola and S. A. Sandford, in *Solid-State Astrophysics*, ed. E. Bussoletti *et al.*, North-Holland, Amsterdam, 1991, p. 29; J. E. Chiar, A. J. Adamson, T. H. Kerr and D. C. B. Whittet, *Astrophys. J.*,

1995, **426**, 240; R. J. A. Grim and J. M. Greenberg, *Astrophys. J. Lett.*, 1987, **321**, 91; J. H. Lacy, F. Baas, L. J. Allamandola, S. E. Persson, P. J. McGregor, C. J. Lonsdale, T. R. Geballe and C. E. P. van de Bult, *Astrophys. J.*, 1984, **276**, 543; S. C. Tegler, D. A. Weintraub, T. W. Rettig, Y. J. Pendleton, D. C. B. Whittet and C. A. Kulesa, *Astrophys. J.*, 1995, **439**, 279; M. E. Palumbo, A. G. G. M. Tielens and A. T. Tokunaga, *Astrophys. J.*, 1995, **449**, 674.

5 L. B. d'Hendecourt and L. J. Allamandola, *Astron. Astrophys. Suppl.*, 1986, **64**, 453; L. J. Allamandola, S. A. Sandford and G. J. Valero, *Icarus*, 1988, **76**, 225; R. J. A. Grim, J. M. Greenberg, M. S. de Groot, F. Baas, W. A. Schutte and B. Schmitt, *Astron. Astrophys. Suppl.*, 1989, **78**, 191; O. M. Shalabiea and J. M. Greenberg, *Astron. Astrophys.*, 1994, **290**, 266.

6 R. E. Johnson, *Energetic Charged Particle Interactions with Atmospheres and Surfaces*, Springer, Berlin, 1990; L. J. Lanzerotti and R. E. Johnson, in *Ion Beam Modifications of Insulators*, ed. P. G. W. Mazzoldi and E. Arnold, Elsevier, Amsterdam, 1987, p. 631.

7 R. E. Johnson, L. J. Lanzerotti and W. L. Brown, *Adv. Space Res.*, 1984, **4**, 41; J. Geiss *et al.*, in *COSPAR Colloquia Series*, ed. E. Marsch and R. Schwenn, Pergamon, New York, 1992, vol. 3, p. 20, and references therein.

8 K. Roessler, in *Solid-State Astrophysics*, ed. E. Bussoletti and G. Strazzulla, North-Holland, Amsterdam, 1991, p. 454.

9 G. Stöcklin, *Chemie heißer Atome*, VCH, Weinheim, 1991.

10 R. I. Kaiser and K. Roessler, *Astrophys. J.*, 1997, **475**, 144; R. I. Kaiser, G. Eich, A. Gabrysch and K. Roessler, *Astrophys. J.*, 1997, **484**, 487; R. I. Kaiser and K. Roessler, *Astrophys. J.*, 1997, submitted.

11 M. Heyl, Report Jül-2409, 1990.

12 W. A. Schutte and J. M. Greenberg, *Astron. Astrophys.*, 1991, **244**, 190, and references therein; R. I. Kaiser, G. Eich, A. Gabrysch and K. Roessler, *Astrophys. J.*, 1997, **484**, 487.

13 E. L. O. Bakes, *The Astrochemical Evolution of the Interstellar Medium*, Twin Press, Vledder, 1997.

14 Z. K. Alksne, A. K. Alksnis and U. K. Dzervitis, *Properties of Galactic Carbon Stars*, Orbit, Malabar, 1991.

15 E. Herbst and W. Klemperer, *Astrophys. J.*, 1973, **185**, 505; E. Herbst, N. G. Adams and D. Smith, *Astrophys. J.*, 1984, **285**, 618; G. Winnewisser and E. Herbst, *Topic Curr. Chem.*, 1987, 121.

16 T. J. Millar and E. Herbst, *Astron. Astrophys.*, 1994, **288**, 561; I. Cherchneff and A. E. Glassgold, *Astrophys. J. Lett.*, 1993, **419**, 41; E. Herbst, H. H. Lee, D. A. Rowe and T. J. Millar, *Mon. Not. R. Astron. Soc.*, 1994, **268**, 335.

17 D. Husain, *J. Chem. Soc., Faraday Trans.*, 1993, **89**, 2164; D. C. Clary, N. Haider, D. Husain and M. Kabir, *Astrophys. J.*, 1994, **422**, 416.

18 R. D. Levine and R. B. Bernstein, *Molecular Reaction Dynamics and Chemical Reactivity*, Oxford University Press, Oxford, 1987.

19 I. R. Sims *et al.*, *J. Chem. Phys.*, 1994, **100**, 4229; I. R. Sims *et al.*, *J. Chem. Phys.*, 1992, **97**, 8798; I. R. Sims *et al.*, *Chem. Phys. Lett.*, 1993, **211**, 461; I. R. Sims *et al.*, *J. Chem. Soc., Faraday Trans.*, 1994, **90**, 1473.

20 Y. T. Lee, *Science*, 1987, **236**, 793.

21 C. Ochsenfeld, R. I. Kaiser, A. G. Suits, Y. T. Lee and M. Head-Gordon, *J. Chem. Phys.*, 1997, **106**, 4141.

22 R. I. Kaiser, C. Ochsenfeld, M. Head-Gordon, Y. T. Lee and A. G. Suits, *Science*, 1996, **274**, 1508.

23 R. I. Kaiser, Y. T. Lee and A. G. Suits, *J. Chem. Phys.*, 1996, **105**, 8705.

24 R. I. Kaiser, D. Stranges, Y. T. Lee and A. G. Suits, *J. Chem. Phys.*, 1996, **105**, 8721.

25 R. I. Kaiser, D. Stranges, H. M. Bevsek, Y. T. Lee and A. G. Suits, *J. Chem. Phys.*, 1997, **106**, 4945.

26 R. I. Kaiser, W. Sun, A. G. Suits and Y. T. Lee, *J. Chem. Phys.*, 1997, **107**, 8713.

27 J. Keene, K. Young, T. G. Phillips and T. H. Büttgenbach, *Astrophys. J. Lett.*, 1993, **415**, 131.

28 R. I. Kaiser, C. Ochsenfeld, M. Head-Gordon, Y. T. Lee and A. G. Suits, *Science*, 1996, **274**, 1508.

29 Y. T. Lee, J. D. McDonald, P. R. LeBreton and D. R. Herschbach, *Rev. Sci. Instrum.*, 1969, **40**, 1402.

30 R. I. Kaiser and A. G. Suits, *Rev. Sci. Instrum.*, 1995, **66**, 5405.

31 D. Proch and T. Trickl, *Rev. Sci. Instrum.*, 1989, **60**, 713.

32 G. O. Brink, *Rev. Sci. Instrum.*, 1966, **37**, 857.

33 N. R. Daly, *Rev. Sci. Instrum.*, 1960, **31**, 264.

34 M. S. Weiss, PhD Thesis, 1986, University of California, Berkeley.

35 M. Vernon, PhD Thesis, 1981, University of California, Berkeley.

36 R. I. Kaiser, C. Ochsenfeld, M. Head-Gordon and Y. T. Lee, *Science*, submitted.

37 W. B. Miller, S. A. Safron and D. R. Herschbach, *Discuss. Faraday Soc.*, 1967, **44**, 108, 291.

38 R. I. Kaiser, A. Mebel and Y. T. Lee, *J. Chem. Phys.*, to be submitted.

39 The zero-point corrections have been calculated for 1-C_3D, C_2HD at the CCSD(T) (coupled cluster singles and doubles with a perturbative treatment of triple excitations) approximation using a TZP (triple zeta polarization) basis set. For c-C_3D the EOMIP-CCSD/TZP (equation of motion CCSD for ionized states) approach was used (R. J. Bartlett and J. F. Stanton, in *Reviews of Computational Chemistry*, ed. K. B. Lipkowitz and D. B. Boyd, VCH, New York, 1990, p. 65.

40 P. Thaddeus *et al.*, *Astrophys. J. Lett.*, 1997, **176**, 73.

41 Y. C. Minh, L. M. Ziurys, W. M. Irvine and D. McGonagle, *Astrophys. J.*, 1991, **366**, 192.

42 E. Herbst, personal communication, 1997.

43 H. Habara, S. Yamamoto, C. Ochsenfeld, M. Head-Gordon, R. I. Kaiser and Y. T. Lee, *J. Chem. Phys.*, to be submitted.

44 E. C. Sutton, R. Peng, W. C. Danchi, P. A. Jaminet, G. Sandell and A. P. G. Russel, *Astrophys. J. Suppl.*, 1995, **97**, 455; F. Combes, G. Wlodarczak, P. Encrenaz and C. Laurent, *Astron. Astrophys.*, 1992, **253**, L29.

45 T. J. Millar, P. R. A. Farquhar and K. Willacy, *Astron. Astrophys. Suppl.*, 1997, **121**, 139.

46 P. Thaddeus, J. M. Vritilek and C. A. Gottlieb, *Astrophys. J. Lett.*, 1985, **299**, 63; H. E. Matthews and W. M. Irvine, *Astrophys. J. Lett.*, 1985, **298**, 61.

47 S. Green, *Astrophys. J.*, 1980, **240**, 962; B. E. Turner, *Astrophys. J. Lett.*, 1989, **347**, L39; P. Thaddeus, J. M. Vrtilek and C. A. Gottlieb, *Astrophys. J. Lett.*, 1985; **299**, 63; T. B. Kuiper, J. B. Whiteoak, R. S. Peng, W. L. Peters III and J. E. Reynolds, *Astrophys. J. Lett.*, 1993, **416**, 33.

48 B. E. Turner, L. J. Rickard and L. P. Xu, 1989, **344**, 292.

49 J. Cernicharo *et al.*, *Astrophys. J. Lett.*, 1991, **368**, 39.

50 S. C. Madden, in *Chemistry in Space*, ed. J. M. Greenberg and V. Pironello, Kluwer, Dordrecht, 1991, p. 437 and references therein.

51 S. Yamamoto and S. Saito, *Astrophys. J. Lett.*, 1990, **363**, 13.

52 C. Ochsenfeld, R. I. Kaiser, A. G. Suits, Y. T. Lee and M. Head-Gordon, *J. Chem. Phys.*, 1997, **106**, 4141.

53 A. Mebel, personal communication, 1997.